Check for updates

Received: 16 February 2021 | Accepted: 25 October 2021

DOI: 10.1111/1365-2435.13966

Functional Ecology | BRITISH ECOLOGICAL SOCIETY

RESEARCH ARTICLE

Host–parasite dynamics shaped by temperature and genotype: Quantifying the role of underlying vital rates

Marjolein Bruijning[1,2] | Erlend I. F. Fossen[3,4] | Eelke Jongejans[2,5] | Héléne Vanvelk[6] | Joost A. M. Raeymaekers[7] | Lynn Govaert[6,8,9] | Kristien I. Brans[6] | Sigurd Einum[3] | Luc De Meester[6,10,11]

[1]Department of Ecology and Evolutionary Biology, Princeton University, Princeton, NJ, USA; [2]Department of Animal Ecology and Physiology, Radboud University, Nijmegen, The Netherlands; [3]Centre for Biodiversity Dynamics, Department of Biology, NTNU, Norwegian University of Science and Technology, Trondheim, Norway; [4]Animal Ecology, Department of Ecology and Genetics, Uppsala University, Uppsala, Sweden; [5]Animal Ecology, NIOO-KNAW, Wageningen, The Netherlands; [6]Laboratory of Aquatic Ecology, Evolution and Conservation, KU Leuven, Leuven, Belgium; [7]Faculty of Biosciences and Aquaculture, Nord University, Bodø, Norway; [8]Department of Evolutionary Biology and Environmental Studies, University of Zurich, Zürich, Switzerland; [9]Department of Aquatic Ecology, Eawag, Swiss Federal Institute of Aquatic Science and Technology, Dübendorf, Switzerland; [10]Leibniz Institüt für Gewasserökologie und Binnenfischerei (IGB), Berlin, Germany and [11]Institute of Biology, Freie Universität Berlin, Berlin, Germany

Correspondence
Marjolein Bruijning
Email: mbruijning@princeton.edu

Funding information
Fonds Wetenschappelijk Onderzoek, Grant/Award Number: G0B9818 and G0C3818; Research Council of Norway, Grant/Award Number: 223257/F50 and 230482; NWO Rubicon, Grant/Award Number: 019.192EN.017; KU Leuven Research Council, Grant/Award Number: C/2017/002; University of Zurich Research Priority Program

Handling Editor: Katie Marshall

Abstract

1. Global warming challenges the persistence of local populations, not only through heat-induced stress, but also through indirect biotic changes. We study the interactive effects of temperature, competition and parasitism in the water flea *Daphnia magna*.
2. We carried out a common garden experiment monitoring the dynamics of *Daphnia* populations along a temperature gradient. Halfway through the experiment, all populations became infected with the ectoparasite *Amoebidium parasiticum*, enabling us to study the interactive effects of temperature and parasite dynamics. We combined Integral Projection Models with epidemiological models, parameterized using the experimental data on the performance of individuals within dynamic populations. This enabled us to quantify the contribution of different vital rates and epidemiological parameters to population fitness across temperatures and *Daphnia* clones originating from two latitudes.
3. Interactions between temperature and parasitism shaped competition, where Belgian clones performed better under infection than Norwegian clones. Infected *Daphnia* populations performed better at higher than at lower temperatures, mainly due to an increased host capability of reducing parasite loads. Temperature strongly affected individual vital rates, but effects largely cancelled out on a population-level. In contrast, parasitism strongly reduced fitness through consistent negative effects on all vital rates. As a result, temperature-mediated parasitism was more important than the direct effects of temperature in shaping population

This is an open access article under the terms of the Creative Commons Attribution License, which permits use, distribution and reproduction in any medium, provided the original work is properly cited.
© 2021 The Authors. *Functional Ecology* published by John Wiley & Sons Ltd on behalf of British Ecological Society.

dynamics. Both the outcome of the competition treatments and the observed extinction patterns support our modelling results.
4. Our study highlights that shifts in biotic interactions can be equally or more important for responses to warming than direct physiological effects of warming, emphasizing that we need to include such interactions in our studies to predict the competitive ability of natural populations experiencing global warming.

KEYWORDS
competition, *Daphnia*, demographic modelling, global warming, host–parasite dynamics, population model

1 | INTRODUCTION

Climate change challenges the persistence of local populations (Bellard et al., 2012). Not only do populations have to cope with changes in temperature, they also face temperature-mediated changes in their biotic environment (Ficke et al., 2007; Gilman et al., 2010; Tylianakis et al., 2008; Urban et al., 2016). For instance, temperature alters host–parasite interactions, both through interactive effects of temperature and parasitism on host performance (Greenspan et al., 2017; Hector et al., 2019; Padfield et al., 2020), as well as through temperature effects on parasite dynamics themselves (Cohen et al., 2019; Gehman et al., 2018; Morley & Lewis, 2014). Depending on how these thermal effects play out in a specific system, where both hosts and their parasites typically show unimodal responses to temperature (Dell et al., 2011; Kirk et al., 2018; Mordecai et al., 2019; Shocket et al., 2019), infections may become more prevalent and more severe under climate change in some systems (Altizer et al., 2013; Hall et al., 2006; Harvell et al., 2002; Lafferty, 2009; Lafferty & Mordecai, 2016; Mouritsen et al., 2005). This could threaten the persistence of natural populations even more than previously believed (Pounds et al., 2006; Harvell et al., 2002; Labaude et al., 2017; Mokany et al., 2019). In addition, as individuals migrate to follow shifts in temperature (Hickling et al., 2006; Thomas & Lennon, 1999), there might be an increasing likelihood that local populations will interact with conspecific immigrants that are pre-adapted to warming (Urban et al., 2012). These immigrants could potentially out-compete local populations, although their success will also depend on the evolutionary potential of the resident population (Van Doorslaer, Vanoverbeke, et al., 2009) and the degree to which immigrant genotypes are adapted to local environmental conditions (De Meester et al., 2018).

Yet, although the importance of biotic interactions for species performance and distributions is well known (Araújo & Luoto, 2007; Gilman et al., 2010; Heikkinen et al., 2007), biotic changes are rarely taken into account when predicting population responses to climate change, and this might explain the general low accuracy in predicting consequences of climate change (Araújo & Luoto, 2007; Gilman et al., 2010). Understanding and predicting how natural populations will respond to multiple environmental stressors simultaneously is considered as one of the most pressing challenges in conservation biology (Schäfer & Piggott, 2018).

Meeting this challenge requires an understanding of how individual vital rates (survival, growth and reproduction) respond to changes in temperature and associated biotic conditions, and how these vital rates together determine population fitness. Not all vital rates have equally large effects on population fitness (Caswell, 1978) and different fitness components can covary positively or negatively (e.g. through trade-offs, Stearns, 1989). Integral Projection Models (IPMs) are useful for integrating over multiple vital rates (Easterling et al., 2000; Ellner et al., 2016; Ellner & Rees, 2006; Merow et al., 2014), and are typically used to quantify the contribution of various vital rates and eco-evolutionary processes to population-level dynamics. IPMs have been parameterized for natural plant (Bruijning et al., 2017; Metcalf et al., 2008; Salguero-Gomez et al., 2012) and animal (Childs et al., 2016; Coulson et al., 2011; Ozgul et al., 2010; Traill et al., 2014; Vindenes & Langangen, 2015) populations, as well as for laboratory systems (Bruijning, ten Berge, et al., 2018; Ozgul et al., 2012; Smallegange & Ens, 2018). Enabled by the flexibility of IPMs, recent years have seen an exciting development of combining IPMs with existing frameworks such as quantitative genetics (Coulson et al., 2017) and dynamic energy budget theory (Smallegange et al., 2017). In this study, we combine IPMs with epidemiological models (Metcalf et al., 2016; Wilber et al., 2016) in order to simultaneously track the dynamics of multiple host genotypes and their parasite.

The aim of our study is to disentangle how latitude-specific host performance is affected by changes in temperature directly and by changes in temperature-mediated parasitism, and to quantify the underlying vital rates and epidemiological rates through which this occurs. The water flea *Daphnia magna*, a small crustacean, is a keystone species in freshwater systems and an excellent model species to study temperature-dependent disease dynamics (Hall et al., 2006; Kirk et al., 2018, 2020; Shocket et al., 2018). An increasing number of studies have shown within-population genetic variation in *Daphnia* in thermal performance (Bruijning, ten Berge, et al., 2018; Van Doorslaer, Stoks, et al., 2009) enabling rapid evolutionary

responses to temperature, as well as among-population genetic variation and local adaptation to temperature (Brans et al., 2017; Geerts et al., 2015; Yampolsky et al., 2014). In addition, natural zooplankton populations generally show high parasite infection rates (Chiavelli et al., 1993; Decaestecker et al., 2004; Stirnadel & Ebert, 1997), and responses to parasites can differ greatly among genotypes (Carius et al., 2001). These host–parasite interactions have the potential to influence the ecological and evolutionary dynamics of host populations (Decaestecker et al., 2007; Ebert, 2005). Studying how infection by parasites and temperature interact to determine population dynamics, via its underlying vital rates, is important, as we hypothesize that both stressors strongly differ in how they impact vital rates. We hypothesize the effects of temperature to be vital rate dependent, with higher temperatures reducing survival, while increasing development rates. On a population level, we expect these opposite temperature effects to partly balance out, as long as temperatures remain below the maximum tolerated temperatures, resulting in relatively weak fitness responses to temperature. On the other hand, because of its expected consistent negative effects on both host reproduction (Decaestecker et al., 2005; Ebert, 2005) and survival (Ebert et al., 2000; Ebert, 2005), we expect parasitism to strongly reduce population fitness. Here, we expect tolerance to differ among genotypes (Figure 1; Carius et al., 2001; Ebert, 2005; Little et al., 2010; Råberg et al., 2007). We expect heat stress to reduce an individual's ability to cope with infection (Hector et al., 2019), acting through multiple vital rates. Finally, temperature-mediated changes in parasite resistance (Figure 1) could even further intensify the severity of infection at higher temperatures, but could also reduce the impact, if temperature exceeds optimum temperatures of the parasite (Gehman et al., 2018; Kirk et al., 2020; Mordecai et al., 2019; Shocket et al., 2019).

To test these hypotheses, we performed a semi-controlled common garden laboratory experiment, monitoring the dynamics of *Daphnia* populations along a temperature gradient. We collected individual life-history data from individuals embedded in their population, letting the populations develop naturally without interfering. This enabled the estimation of density dependence in life-history features (Bruijning, ten Berge, et al., 2018). In addition to single-clone populations, we followed dynamics when clones from four ponds, located at two different latitudes, were put together, reflecting a scenario in which local individuals face immigrants. The occurrence of a spontaneous infection with a generalist ectoparasite *Amoebidium parasiticum* in all experimental units halfway through the experiment gave us the opportunity to quantify clone and temperature-specific tolerance and resistance against infection. We used the collected data on individuals embedded

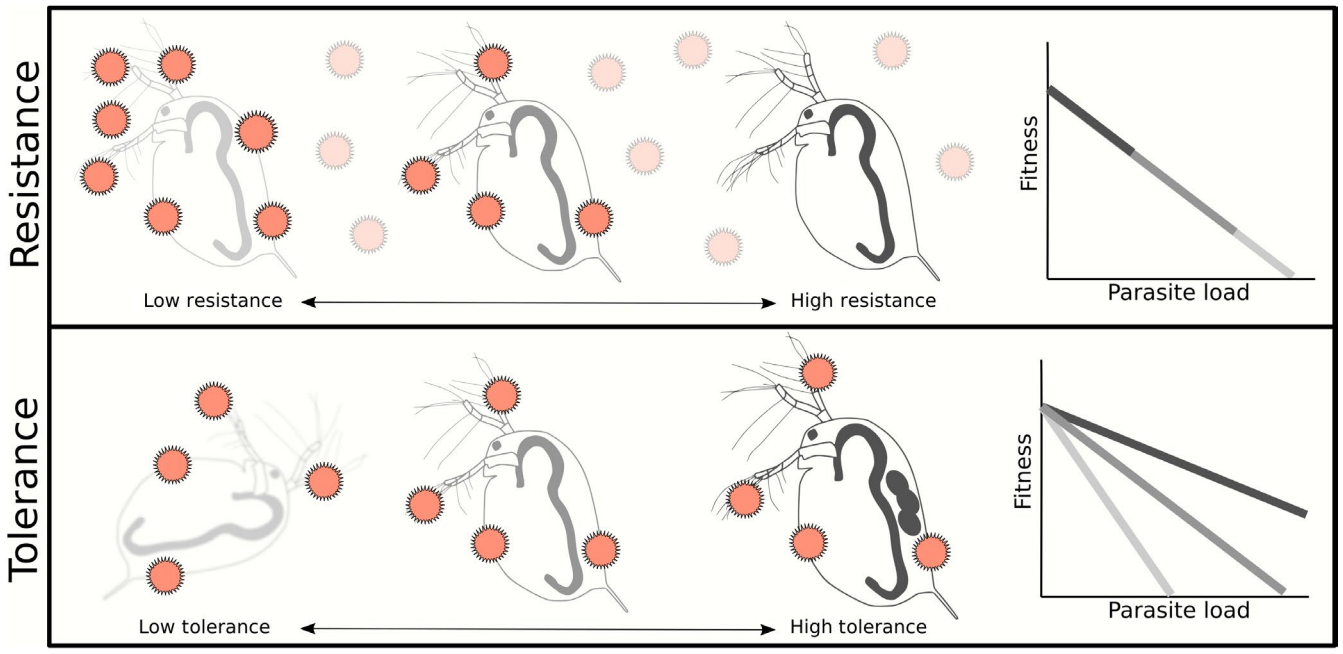

FIGURE 1 Schematic overview illustrating the concept of parasite resistance and parasite tolerance. Different greyscales depict different host genotypes. Upper row shows variation in parasite resistance, which is defined as the ability of an individual to limit parasite burden (Råberg et al., 2007). Each genotype experiences the same parasite exposure, but differs in its parasite load. The light grey genotype has the lowest resistance, on a population level resulting in the highest average parasite loads (and thus lowest fitness), while the dark grey genotype has the highest resistance. Bottom row shows variation in parasite tolerance, defined as the ability of the host to limit negative effects of the parasite (Råberg et al., 2007). Note that tolerance can either be measured as a mean, comparing fitness for a given parasite burden (point tolerance), or as the slope, comparing how strongly fitness declines with increases in parasite burden (range tolerance; Little et al., 2010). In the example shown here, the two measures agree on the relative tolerance of each genotype, but this is not necessarily the case. The light grey genotype has the lowest tolerance (therefore here shown to be unable to survive), while the dark grey genotype has the highest tolerance (here shown to carry eggs and reach a larger body size). Both high resistance and high tolerance can, in isolation or in combination, help hosts to defend themselves against parasites (Råberg et al., 2007)

in populations to parameterize a temperature-dependent host–parasite IPM, capturing temperature-dependent dynamics in both hosts and their pathogen, as well as interactions between hosts and parasites. Both our empirical observations and our modelling results indicate that temperature-mediated parasitism was profoundly more important than direct temperature effects in shaping host fitness. This underscores that, in order to successfully predict biological responses to global warming, we need to include temperature-mediated changes in biotic interactions in our studies.

2 | MATERIALS AND METHODS

For a more detailed description of the methods, see Appendix S1. The main aspects of our experiment and analyses are explained below.

2.1 | Data collection

2.1.1 | Experimental design

We used resting eggs of *D. magna* originating from four fishless ponds, two located in Belgium (which we refer to as B1 and B2) and two located nearby Trondheim, Norway (N1 and N2). These resting eggs were hatched in the laboratory to establish clonal lineages. From each pond, we arbitrarily selected three clonal lineages, resulting in a total of 12 clones ($N1_{A-C}$, $N2_{A-C}$, $B1_{A-C}$, $B2_{A-C}$). The study did not require fieldwork permission or ethical approval.

Four experimental temperatures were established using temperature-controlled water baths (±0.5°C): 14, 18, 22 and 26°C. We followed single clone as well as mixed populations. Every clone was exposed to each of the four temperatures, resulting in 48 single-clone populations. For the mixed populations, we created each two-clone combination once, and distributed clones equally across the three highest temperatures. This resulted in 66 unique temperature × clonal mixture combinations, in total resulting in 114 populations.

The experiment lasted 81 days (see Appendix S2 for a timeline). We started each population with 12<24 hr old neonates (from clutch 2–5; either 12 neonates from the same clone, or 6 neonates from each of the two clones). During the first week, individuals were kept in 500-ml jars filled with dechlorinated tap water. After that, populations were transferred to 1.5-L aquaria. In each aquarium, we placed two transparent tubes (4 cm diameter), containing 12 holes covered with a 125-μm plankton gauze allowing medium (water and food) to pass, but preventing exchange of *Daphnia*. These tubes enabled us to measure the performance of isolated individuals, while they were still part of the population (see below, and Bruijning, ten Berge, et al., 2018). Populations were kept in dechlorinated tap water and fed daily 0.1 ml Shellfish Diet 1800® L^{-1} medium. Food was added both to the aquaria and to the tubes at equal concentrations. Twice per week, the medium was partially refreshed, keeping 0.5 L of the old medium.

2.1.2 | Population and individual measurements

All units were measured twice a week, with 3- or 4-day intervals. For each unit, we made a short movie of the population (set-up details in Czypionka et al., 2016), in order to obtain population size estimates, using the R package TRACKDEM (Bruijning, Visser, et al., 2018). For each of the individuals isolated in the tubes, we noted whether the individual was alive, its size (carapace length [mm], measured from the middle of the eye to the base of the tail using a stereomicroscope), the number of eggs in the brood pouch and the number of produced neonates. If neonates were produced, we measured the size of one of the neonates. The individuals and neonates that were in the tube were either put back in the population or sampled for genetic analysis (see Section 2.1.4). Two new individuals, one juvenile and one adult, were then arbitrarily picked from the population. We measured their size, counted the number of eggs in the brood pouch and placed them in the tubes.

2.1.3 | Parasite load

After an initial increase in population abundance in all aquaria, all populations strongly declined in size during the second half of the experiment (Figure 2a). On day 60, we noted that the cultures were spontaneously infected by the ectoparasite *A. parasiticum*. Infection with this laboratory-borne parasite has been observed before, and typically occurs during the fall. We therefore anticipated that infection could occur. From day 60 onwards, we scored the parasite load for each measured individual, on a 0–3 scale (0: no signs of infection; 3: heavily infected). This was done both when first measuring the individual and when measuring it again after 3 or 4 days. To reconstruct the dynamics of the infection before day 60, we scored parasite loads afterwards for a subset of individuals ($n = 654$) that had been sampled for genetic analysis and stored in ethanol. In this procedure, we scored individuals going back from day 60 until day 38. For those populations in which at least one of the sampled individuals was infected at day 38 (which was the case in 10% of the populations), we continued to score individuals from earlier days, until only uninfected individuals were observed. The first infected individual was observed at day 29. We set parasite load for all populations before day 29 and for all unchecked populations before day 38 at zero.

2.1.4 | Genetic analyses

To identify genotypes in the competition treatments, we sampled individuals during the experiment for which we obtained demographic data. This sampling was started at day 17, when the initial cohort had produced their first clutches across all temperature treatments.

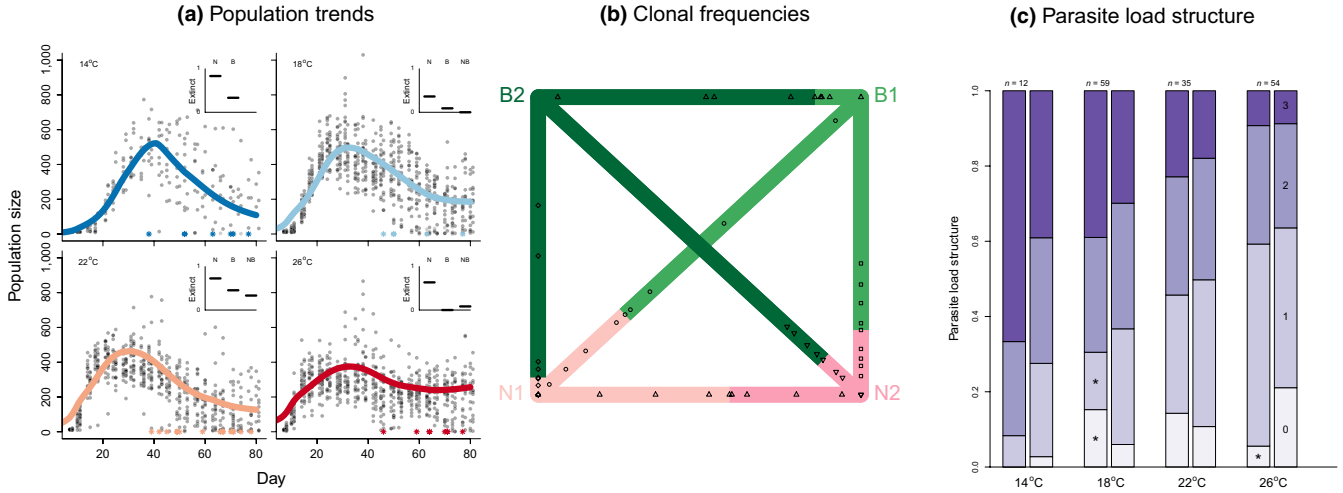

FIGURE 2 Population-level observations on population numbers (a), genotype frequencies (b) and parasite load structure (c). (a) Observed population sizes over time per temperature, across all clonal treatments. Dots indicate observed population sizes estimated using R package TRACKDEM (Bruijning, Visser, et al., 2018). Lines indicate projections based on the constructed IPMs, using day-specific observed population sizes to project 1 day ahead. Here, we averaged projections across the four locations. Insets show the proportion of populations that went extinct during the experiment: N indicates populations consisting of one or two Norwegian clones, B indicates populations consisting of one or two Belgian clones and NB indicates populations consisting of one Belgian and one Norwegian clone. Note that at 14°C there were only single-clone populations. Asterisks at the bottom of each graph indicate extinction occurrences through time. In total, 62% of the Norwegian, 21% of the Belgian and 14% of the mixes went extinct prior to the end of the experiment. (b) Clonal frequencies for each pairwise combination, based on all sampled individuals during the experiment. Coloured lines (two hues of pink for the two Norwegian and two hues of green for the two Belgian clones) indicate the median proportion across all relevant populations. Dots indicate proportions for each of the populations. Note that we tested three genotypes per location, and each dot shows results for a unique combination of two genotypes. (c) Observed parasite load structure (left bars) compared to predicted parasite load structure (right bars) at the end of the experiment (days 80–81). Darker colours indicate higher parasite load classes. To obtain predictions, we used the fitted parasite transition matrix (see Appendix S1.2) to project how parasite load structure changes through time, keeping total population sizes equal (i.e. ignoring host demography). Asterisks indicate those cases where the observed proportions did not fall within 95% of simulated values, when sampling parasite load classes from a multinomial distribution based on the predicted proportions (see Appendix S4.2 for more details)

In total, we sampled 1,676 individuals from those competition treatments that contained between-population combinations (e.g. $N1_A$–$N2_A$). We used a total of nine microsatellite markers to identify genotypes (Orsini et al., 2012). DNA was extracted using the NucleoSpin® 96 Tissue Core Kit. Results were manually scored using software GeneMarker®.

2.2 | Modelling framework

2.2.1 | Vital rate fitting

In our dataset, there are 14% missing data for observations on parasite score, 16% missing data on genotype and 0.5% missing data on population density. We imputed these missing observations by multiple imputation by chained equations, using R package MICE (van Buuren & Groothuis-Oudshoorn, 2011), creating 10 imputed datasets. These datasets were subsequently used to fit vital rate models, defining six vital rates: survival, growth, probability of carrying eggs, probability of producing offspring (conditional on carrying eggs; measuring neonate development rate), clutch size and offspring size.

Per vital rate, we fitted GLMs including additive effects of initial body size (z), squared body size (z^2), temperature (T), squared temperature (T^2), population density (N), parasite score (P) and location of origin (L). We combined data on single-clone treatments and competition treatments, as preliminary analyses did not show strong effects of competition. While we did experiments with three genotypes per population, we fitted our models using location of origin (i.e. population) as the lowest level of resolution. In addition, to test for differential responses across locations, we included two-way interactions between location L and z, T, N and P. Finally, we included an interaction between temperature and parasite load. The most complex model contained 23 parameters. We tested different models, and continued with the model resulting in the lowest average *AIC* across the 10 imputed datasets (results in Appendix S3). Coefficients and variances were averaged across these 10 models, taking into account both the between-imputation variance and the variance associated with each parameter (Yuan, 2000).

2.2.2 | Construction of two-state IPMs

We used IPMs to integrate over the six vital rates. IPMs describe the dynamics of a population in which individuals are characterized by a continuous state variable (body size z in our case), in discrete time (Easterling et al., 2000; Ellner et al., 2016; Ellner

& Rees, 2006; Merow et al., 2014). We use a time step of 1 day, which is short compared to the life span of individuals. We created an IPM that was additionally a function of temperature, density, population origin and parasite load, and discretized this IPM, as is standard practice (Easterling et al., 2000; Merow et al., 2014), into a 100 × 100 matrix.

We then combined this IPM with a host–parasite model, in order to concurrently track dynamics of both body size and parasite load distributions. We use a discrete-time epidemiological model (e.g. Bjørnstad et al., 2002; Oli et al., 2006) that describes how the number of susceptible and infected hosts in a population change through time, based on transition probabilities between epidemiological compartments (i.e. transmission and recovery rates). We defined three infected states, corresponding to the measured three levels of parasite load, and estimated transition probabilities between all four parasite load classes (0: uninfected/susceptible; 1–3: levels of infection).

Amoebidium parasiticum reproduces by the production of spores (Kuno, 1973) that can remain viable for a long time (Decaestecker et al., 2004; Ebert, 1995). As we kept one third of the old medium when cleaning the aquaria twice a week, there might have been a build-up of spores in the aquaria through time. This is supported by the observation that average parasite loads continued to increase with time irrespective of density declines (Figure 5), and that only a few populations had substantial levels of recovery. We therefore decided to model infection probabilities α as a function of the population-level average parasite load ($\overline{P}_t$): $\alpha_t = 1 - \exp\left(-\beta\overline{P}_t\right)$. Note that it is thus not a function of temperature. Transition probabilities γ (parasite load increase), ω (parasite load reduction) and ρ (recovery) were fitted as a function of temperature, as observations show temperature dependence in parasite dynamics (Figure 5). A logit link function was used to obtain probabilities. We included two sources of data to estimate these parameters: (a) Individual observed transitions in parasite load, and (b) population-averaged parasite loads over time, calculated per temperature. We optimized the log likelihood comparing predictions to observations. For this analysis, we made the simplifying assumption that all aquaria, across all temperatures, were exposed to the parasite on the same day, based on the observation that populations started to crash around the same time. We set this day at day 29, as this is when we observed the first infected individual. We performed sensitivity analyses to assess the robustness of our parameters and conclusions against the set start day of infection, and against temporal variation in onset across temperatures (more details and results in Appendix S4).

The discretized body size-structured IPM (being a function of *N*, *P*, *L* and *T*), and the estimated parasite transition matrix were combined into a two-state IPM, which described all transitions between body sizes, as well as all transitions between parasite load classes. Here we assume that neonates are born uninfected, but results remain essentially identical when we instead assume that neonates are born with the same parasite load as their mother (results not shown). The resulting 400 × 400 matrix was used for subsequent analysis.

2.2.3 | Temperature-mediated host–parasite dynamics

We performed three analyses to assess how host–parasite dynamics were affected by temperature and clonal background. First, the one-state IPM was used to project asymptotic population growth rates (λ; defined by the largest eigenvalue of the discretized matrix) for different densities, temperatures, parasite scores and locations. By assessing at which density, population growth rate equalled 1 (indicating a stable population), we obtained projected equilibrium densities as a measure for performance. We did this for all combinations of the four populations of origin, temperatures and parasite score.

Second, we quantified the relative effect of temperature increases, parasitism and their interaction. We calculated proportional changes in each vital rate when increasing temperature from either 16°C to 21°C or from 21 to 26°C, increasing parasite load from 0 to 1, and increasing both temperature and parasitism. We then calculated how these effects on each of the vital rates affected projected equilibrium densities, based on the one-state IPM. Effects were averaged across the four locations.

Third, we used the two-state IPM to quantify how different vital and epidemiological rates contributed to differences in host–parasite dynamics at 16°C compared to 21°C, and at 21°C compared to 26°C. Per location, we first projected the stable parasite load structure and host equilibrium density at either 16 or 21°C, by projecting dynamics for 200 time steps. We then replaced different rates by the rates when temperature was set at either 21 or 26°C, and projected parasite load structure and equilibrium density again. These rates were the transition probabilities between parasite classes (ρ, γ, ω) and the host's demographic responses to temperature, in interaction with parasite infection. We here separated the combined effects through survival and growth, and the combined effects through reproduction and neonate body size.

3 | RESULTS

3.1 | Observed population trends and genotype frequencies

After a strong increase in densities in all 114 populations, all populations showed strong reductions in size during the second half of the experiment (Figure 2a), at all temperatures. Genetic analyses indicated that in the mixed populations, the Belgian clones (both B1 and B2) out-competed Norwegian clones (both N1 and N2), and that clones from B2 largely out-competed those of B1 (Figure 2b). This is in agreement with the extinction patterns: 62% of the Norwegian, 21% of the Belgian and 14% of the Norwegian–Belgian mixed

populations went extinct (Figure 2a). Nearly all extinctions occurred after day 40 (Figure 2a), which was after the initial spread of the parasite.

3.2 | Model validation

We performed four checks to confirm that our parameterized modelling framework adequately describes observed vital rates, parasite load structures, population trends, as well as competition outcomes. First, the vital rate models resulted in unbiased predictions across all parasite loads (Appendix S5.1). Second, temperature-specific predictions on parasite load distributions at the end of the experiment captured the observed dynamics fairly well (Figure 2c; Appendix S5.2). Third, the two-state IPM resulted in reasonable daily population-level projections (Figure 2a), but slightly overestimated population growth. The average difference between daily predicted and observed changes in population size, averaged across all treatments, was 9%; we note that our IPM projections did not include any demographic stochasticity, which would likely lower projected population growth. Fourth, simulated clonal frequencies, based on two-state IPM projections in which we let two clones compete, closely resembled observed clonal frequencies for all combinations (Appendix S5.3). Altogether, these analyses gave us confidence that the parameterized host–parasite IPM adequately describes the observed dynamics, and that it can thus be used to quantify the processes underlying these dynamics.

3.3 | Single vital rates

All estimated coefficients can be found in Appendix S6. Body size had significantly positive effects on the probability of carrying eggs, the number of eggs produced and the size of the neonates, and negative effects on somatic growth. Temperature had positive effects on vital rates associated with reproduction, but negative effects on survival. We found a negative temperature-squared effect in somatic growth and the probability of producing offspring, indicating a unimodal response. Parasite load had negative effects on all vital rates, except on the probability of producing offspring conditional on having eggs. The interaction between parasite load and temperature had a positive effect on the probability of carrying eggs. Population density negatively affected all vital rates, except survival (see Appendix S1.2) and neonate size. All vital rates showed significant effects of genotypes. Coefficients comparing the Norwegian with the Belgian locations showed that Norwegian clones had lower survival, somatic growth and neonate size, while faster neonate development than Belgian clones. Neonate development of the two Norwegian populations responded stronger to the parasite than that of the Belgian populations. Finally, we found a strong genotype × parasite interaction effect for the two Norwegian clones: in three out of six vital rates, clones from population N2 responded stronger to parasite load than N1.

3.4 | Effects of temperature and parasitism

The constructed IPM revealed a strong negative effect of parasite load on projected equilibrium densities, with tolerance varying among locations (Figure 3). We found similar patterns when considering invasion population growth rates (Appendix S7). The effects of temperature were weak compared to the effects of parasitism. Belgian populations were projected to achieve higher densities than Norwegian populations at all temperatures, and across parasite loads. Clones from location N2 were the least tolerant to increasing parasite loads, while clones from location B2 showed the highest tolerance.

At both ends of the tested temperature gradient, increasing temperature led to a small proportional reduction in survival (Figure 4a,c). Although this reduction was small, at the population level it nearly cancelled out the clear-cut positive effects temperature had on vital rates related to reproduction (Figure 4b,d). This is caused by the large sensitivity of equilibrium densities for changes in survival. In contrast, parasitism had consistent negative effects on all vital rates (Figure 4a,c) and, mainly through decreases in survival and somatic growth, strongly reduced projected equilibrium densities (Figure 4b,d).

3.5 | Host–parasite dynamics at different temperatures

Estimated daily infection probabilities (i.e. the daily probability of transitioning from parasite load class 0 to parasite load class 1, $0 \rightarrow 1$; α) increased with increasing population-level average parasite load (Figure 5). Recovery ($1 \rightarrow 0$; ρ), parasite load reduction ($2 \rightarrow 1$, $3 \rightarrow 2$; ω) and parasite load increase ($1 \rightarrow 2$; $2 \rightarrow 3$; γ) probabilities all increased with temperature, with the probability of reducing parasite load (ω) showing the strongest temperature response (Figure 5). The estimated proportion of infected individuals at day 29, when the first infected individual was observed, was 3.4%. Changing the day at which the infection starts in our model does not affect any of our epidemiological rates (Appendix 4). Although we have no indication that the onset of infection varied with temperature, we also performed a robustness check in which we relaxed our assumption on simultaneous parasite exposure at each temperature, and instead assumed systematic differences across temperatures. This extreme scenario leads to weaker thermal responses in terms of estimated recovery and parasite load growth, while the strong positive effect of temperature on parasite load reduction remains (Appendix S4). Across all these analyses, the estimated epidemiological rates result in consistent lower population-average parasite loads at higher temperatures (i.e. higher resistance; Figure 5, Appendices S5.2 and S4).

Finally, per location, we assessed which processes related to tolerance and resistance caused temperature-related differences in host–parasite dynamics. The two-state IPM predicted higher equilibrium host densities and generally lower infection

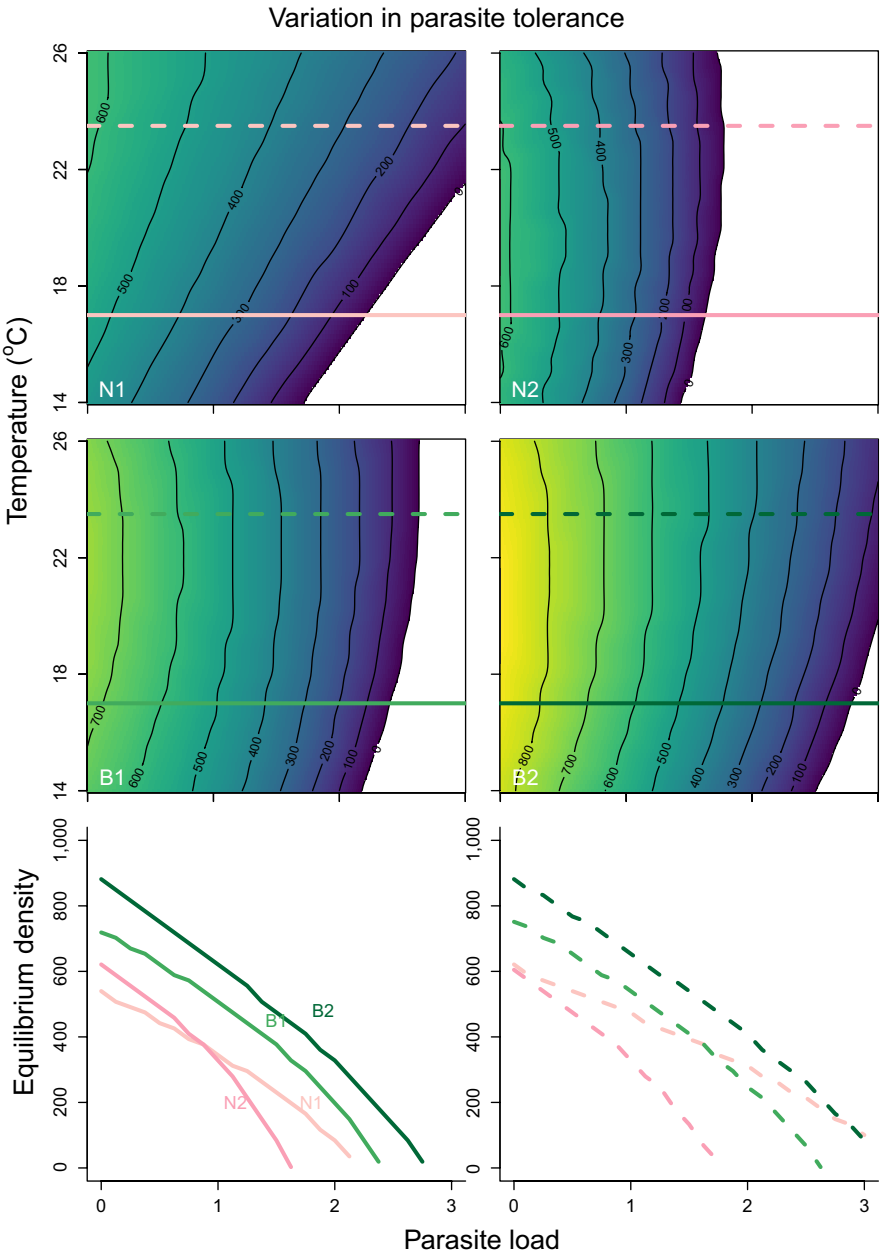

FIGURE 3 Variation in parasite tolerance among the four locations, in interaction with temperature. Landscapes show projected equilibrium densities (as a measure for fitness) for different combinations of temperature and parasite load, based on an integration of all vital rates using Integral Projection Models. Different landscapes show results for different locations of origin. Values smaller than zero are not shown. As these landscapes depict how population fitness decreases with an increasing parasite load, for a given temperature, they show variation in tolerance (see Figure 1). Bottom row shows relation between fitness and parasite load for each location and for two temperatures (as indicated in the panels above)

loads at higher temperatures (Figure 6). This was mostly due to temperature-related differences in resistance, especially the positive temperature effects on daily parasite load reduction and host recovery, which simultaneously decreased parasite load and increased equilibrium host density (pink and green arrows in Figure 6). Parasite load increase, which showed a positive temperature effect (Figure 5), had the opposite effect and reduced equilibrium densities (orange arrows in Figure 6). Finally, temperature-related host tolerance to infection also contributed to the higher population performance at higher temperatures. In particular, hosts from locations N2 and B1 benefited from temperature effects on reproduction and neonate size in terms of equilibrium density (yellow arrows). Temperature effects on host tolerance through survival and growth had smaller and more variable effects across locations (grey arrows).

4 | DISCUSSION

Climate change is predicted to have profound and complex effects on local populations, not only through thermal effects, but also through altered biotic interactions (Hoffmann & Sgrò, 2011; Ockendon et al., 2014; Urban et al., 2016). The results of this study support this idea, as we found strong genotype- and temperature-dependent impacts of an ectoparasite on host performance. By parameterizing a temperature-dependent host–parasite IPM, we gained a more mechanistic understanding in the combined effects of warming and parasitism on *Daphnia* hosts originating from different natural populations. Only by this approach, integrating over all vital and epidemiological rates, we could show how the temperature-dependent effects of parasitism on host performance were much stronger than the direct

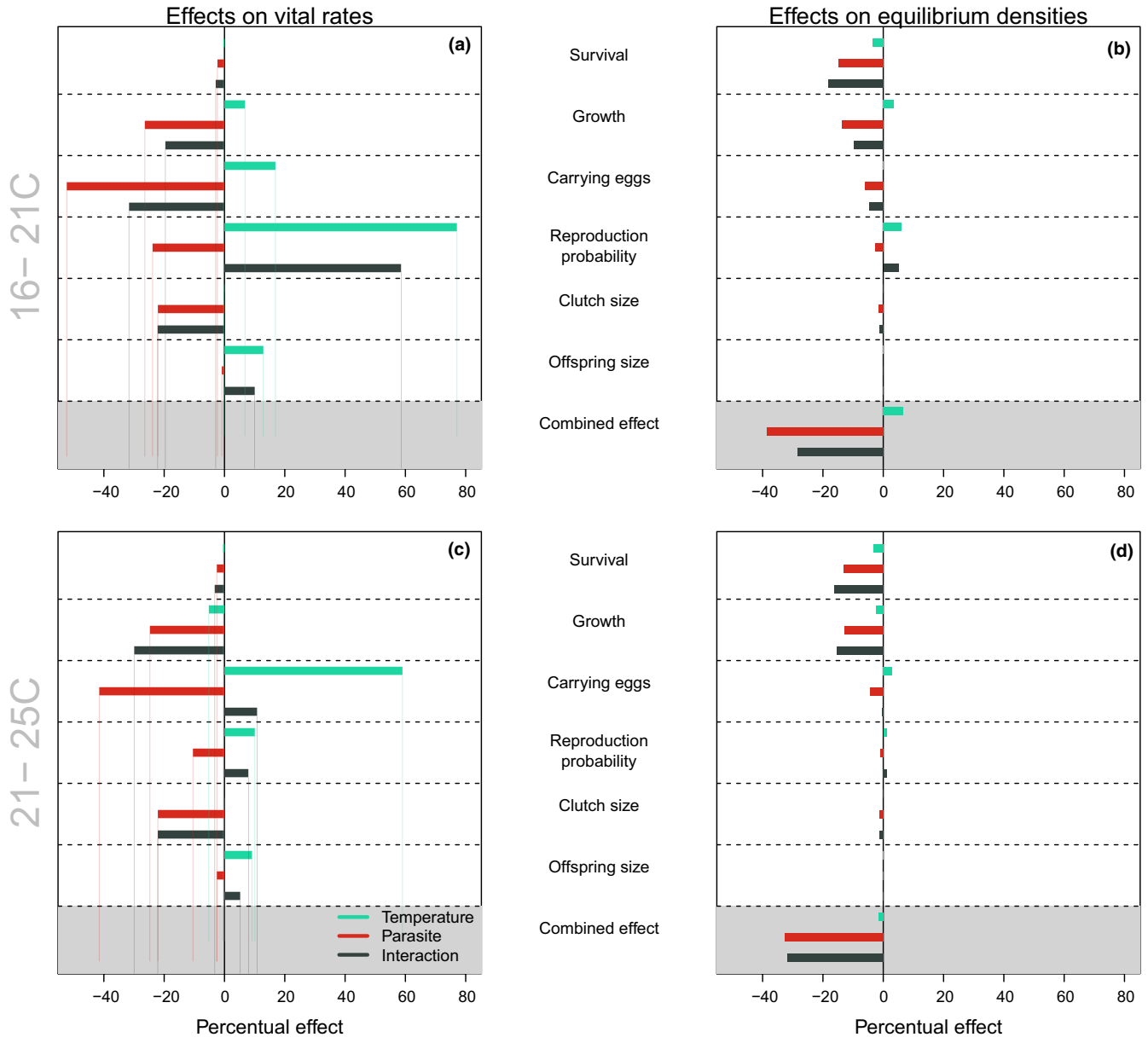

FIGURE 4 Relative effects of temperature (green), parasitism (red) and their interaction (grey) on (a, c) each of the vital rates, and on (b, d) projected equilibrium densities, through effects on each of the vital rates. Temperature effects were calculated by increasing temperature from 16 to 21°C (a, c) and from 21 to 26°C (b, d). We calculated effects of parasitism by increasing parasite load from 0 (i.e. uninfected) to 1 (lowest infected class). For (b, d), we used the one-state IPM to calculate effects on equilibrium densities when one of the vital rates was altered by temperature, parasitism or both. These effects combine the effect sizes shown in (a, c), with the sensitivity in equilibrium densities for changes in that vital rate. Bottom row in (b, d) shows the combined relative effect, that is when all vital rates are altered by temperature, parasitism or both

effects of temperature. This is not due to an absence of temperature effects on individual vital rates, but because higher temperatures had opposing effects on different vital rates, leading to a decrease in survival but an increase in reproduction. These effects largely cancelled out on a population level. In contrast, parasitism had consistently negative effects on all vital rates, strongly reducing population performance (Figures 3 and 4). Furthermore, strong temperature dependence in both host resistance and tolerance (Figures 5 and 6) resulted in indirect temperature effects to be more important in shaping host fitness than direct temperature effects. Finally, as hypothesized, populations differed greatly in their ability to cope with the infection, with the Belgian clones out-competing the Norwegian clones (Figures 2b and 3). Altogether, our results underscore that the consequences of climate change will depend not only on the capability of local populations to respond to changing thermal conditions, but also largely on their capability to respond to associated changes in parasite dynamics, and on their capability to compete with immigrant conspecifics that differ in their responses to temperature and/or parasites.

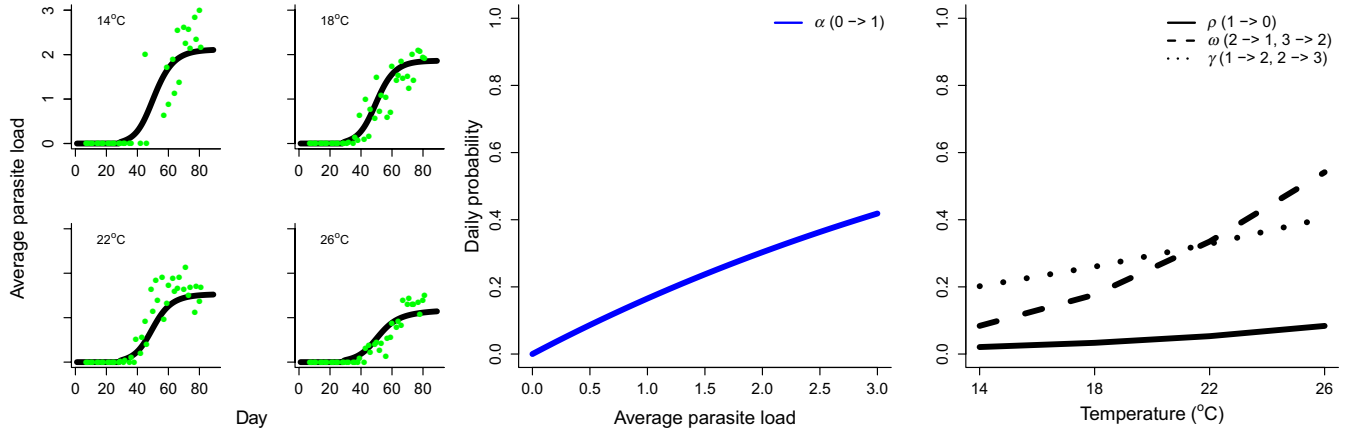

FIGURE 5 Estimated individual probabilities of transitioning between parasite load classes. These rates together shape parasite resistance (see Figure 1), as a function of temperature. Small graphs on the left show, per temperature, predicted parasite loads through time, and green dots show observations averaged over all clonal treatments. Graph in the middle shows (in blue) daily infection probabilities α of individuals (i.e. daily probabilities of transitioning from parasite load class 0 to 1, as indicated in the graph) as a function of the population-level average parasite load. Right graph shows estimated recovery probabilities ρ, probabilities of moving to the previous parasite load class ω and probabilities of moving to the next parasite class γ, as a function of temperature

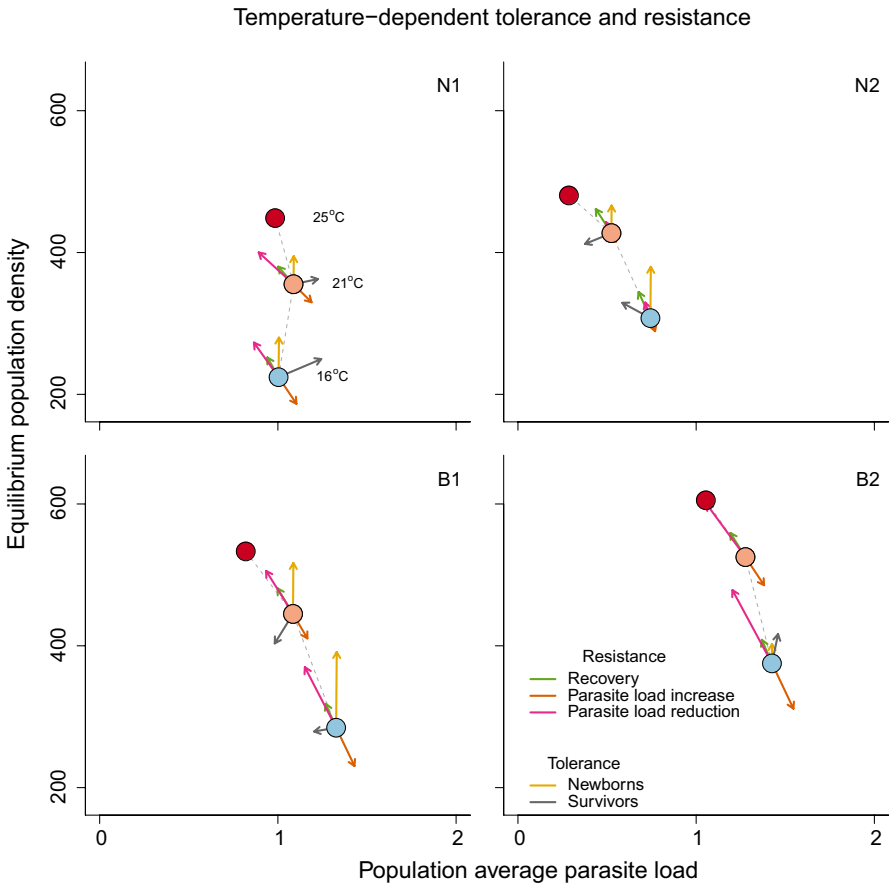

FIGURE 6 Contribution of different processes to temperature-related differences in host–parasite dynamics for each location. Dots show the average population-level parasite load and equilibrium population density after 250 time steps, based on the constructed two-state host–parasite IPM, at 16°C (light blue) and 21°C (orange) and 26°C (red). For all four locations, populations reach higher densities and a lower average parasite load at higher temperatures. Arrows show the contribution of the underlying rates to these effects, by changing functions associated with the host resistance and tolerance, from 14 to 21°C, and from 21 to 26°C

The observed associations between environmental conditions and single vital rates (see Appendix S6) are in line with literature data derived from static life table experiments on *Daphnia* (Giebelhausen & Lampert, 2001; Henning-Lucass et al., 2016; MacArthur & Baillie, 1929; Van Doorslaer, Stoks, et al., 2009): temperature increased vital rates related to development, while it decreased survival. Higher population densities decreased growth and reproduction, but increased neonate size. These are the effects expected from a decrease in per capita food availability (Lampert, 1978); reduced food intake has been shown to increase neonate size in *Daphnia*, increasing their capacity to deal with starvation (Goser & Ratte, 1994; Guisande, 1993). The ectoparasite *A. parasiticum*

negatively affected five out of six vital rates, which is consistent with the observation that, although ectoparasites generally have relatively small effects compared to endoparasites (Decaestecker et al., 2004; Ebert, 2005), they decrease host performance when abundant (Brambilla, 1983; Kuno, 1973; Stirnadel & Ebert, 1997). A resurrection ecology study of Pauwels et al. (2007) suggested a relation between levels of the stress protein *Hsp60* in *Daphnia* and changes in *A. parasiticum* abundance, also indicative of a strong effect of *A. parasiticum* on its host.

Our novel, semi-controlled experimental set-up enabled us to measure temperature and parasite effects on various underlying rates related to host resistance and tolerance, in a way that individuals still experienced ambient population densities. This has the clear advantage that we could simulate natural, density-dependent, dynamics as much as possible, purposefully letting hosts and parasites change dynamically without interfering, while controlling for environmental conditions such as temperature and food. As we did not experimentally control factors such as host density and parasite exposure, inferring precise causal relationships is more difficult than in standard life table experiments. For instance, the spread of infection and the reduction in host population sizes co-occurred, and we therefore do not have data on parasite effects on *Daphnia* populations in their exponential growth phase. Moreover, the start of the infection was uncontrolled, and there could have been some minor variation in the timing of initial infection across aquaria. This might have influenced our estimates of interactive effects of densities, parasite load and temperature that we derived from the data, although we note that (a) our modelling results captured the observed population dynamics of hosts and parasites well (Figures 2 and 5; Appendix S5), and (b) our epidemiological parameters and conclusions are robust against some assumptions we made on the onset of the infection (Appendix S4). Carefully designed future experiments in which both density and parasite exposure are controlled and independently manipulated could further help disentangle causal relationships, complementing our focus on dynamic populations (see Appendix S8 for some other methodological considerations).

Our experimental and modelling approaches, integrating over all vital and epidemiological rates, provided insights into drivers of direct and indirect temperature-mediated effects that could not have been derived from standard life table experiments. Whether or not infections in a specific host system will become more severe under climate change (Altizer et al., 2013; Harvell et al., 2002; Mouritsen et al., 2005) will depend on how sensitive different host and parasite traits are to temperature changes, their respective thermal optima and how the combination of these effects play out for host and parasite fitness in dynamic populations. For instance, Kirk et al. (2020) show how unimodal temperature responses in several *Daphnia* and parasite traits together predict an intermediate temperature where the spread of infection will be most severe. While, in our study, we found some evidence for a thermal optimum within the tested temperature range in two vital rates, on a population-level, there was only a weak direct temperature effect. Disease dynamics responded broadly similar to temperature at both ends of the tested temperature gradient (Figures 4 and 6). In another study, Shocket et al. (2019) nicely illustrate how temperature increases can have contrasting effects on various components of parasite transmission, increasing host–parasite contact while decreasing parasite spore yield. It is these varying sensitivities and potentially contrasting effects that emphasize the importance of integrating single components, in order to quantify how changes in single components translate into changes in population fitness, and to get a more mechanistic understanding in the processes underlying population-level responses.

For the host–parasite interaction studied here, increased temperatures reduced the impact of infection on host fitness. This was mainly due to a temperature dependence in the ability of the host to reduce parasite burden. As *A. parasiticum* is an ectoparasite that attaches to the *Daphnia* carapace, the reduction in parasite loads with increasing temperatures might be related to the moulting frequency. The estimated probability of full recovery, however, was very low, at all temperatures. This is in agreement with the observation that *Daphnia* parasites generally result in chronic infections (Ebert, 2005). To a lesser extent, and contrary to our expectation, we found that hosts showed increased tolerance at higher temperatures, mainly due to a demographic benefit in reproduction. Together, the consistently negative effect of parasitism on all vital rates, with temperature-dependent parasite dynamics, had stronger effects on host fitness than the direct effects of temperature itself. The Belgian clones were able to maintain the highest fitness under parasite exposure (Figures 3 and 6), which is also corroborated by our data on genotype frequencies in competition trials: in almost all combinations, the Belgian clones dominated (Figure 2b; Appendix S4.3). In a scenario of northward migration of the studied Belgian *Daphnia* populations, their enhanced ability to cope with *A. parasiticum* might give them an advantage over the local populations, although future studies should confirm the generality of this statement. Nevertheless, this study clearly shows that accurate predictions of local population responses require taking into account interactions between parasite exposure, temperature and host origin.

There is a pressing need to understand how natural populations will respond to multiple environmental stressors simultaneously (Schäfer & Piggott, 2018; Tekin et al., 2020). We focused on temperature effects on the dynamics of a disease, but a temperature dependency in other biotic factors, such as resources (Huey & Kingsolver, 2019) or predators (Hall et al., 2006), will further shape the fate of natural populations. In the future where the increased occurrence of diseases is predicted to threaten natural as well as agricultural systems, we need to deepen our understanding of mechanistic factors (Altizer et al., 2013). This will require a combination of experimental and theoretical approaches. Experimental approaches as ours have the potential to increase our mechanistic understanding, especially when combined with models that simultaneously track direct and indirect temperature-dependent dynamics in hosts and their parasite. We believe that this provides a powerful way to improve our understanding of how natural populations respond to global warming and its associated biotic and abiotic consequences.

ACKNOWLEDGEMENTS

The authors are very grateful to Peter De Witte, Lotte De Bauw, Hyeun-Ji Lee and Jessie Engelen for helping with the experiment, and to Niels Wagemaker, Pauline van Alebeek and Marta Pineda Gil for helping with the genetic analyses. This experiment was supported by KU Leuven Research Council project C/2017/002, FWO projects G0B9818 and G0C3818, and the Research Council of Norway projects 230482 and 223257/F50. M.B. is funded by NWO Rubicon (019.192EN.017), and L.G. is funded by the University of Zurich Research Priority Program 'URPP Global Change and Biodiversity'.

CONFLICT OF INTEREST

The authors have no competing interests to declare.

AUTHORS' CONTRIBUTIONS

M.B., J.A.M.R., E.J. and L.D.M. conceived the ideas; M.B., E.I.F.F., J.A.M.R., E.J., S.E. and L.D.M. designed the experiment; E.I.F.F. provided the Norwegian clones; K.I.B. provided the Belgian clones; M.B., E.I.F.F. and H.V. collected the data, with regular help of K.I.B. and L.G., and with input of K.I.B. and L.D.M. for troubleshooting; M.B. analysed the data and wrote the first draft of the manuscript, with strong input of L.D.M. and E.J. All authors contributed substantially to further versions of the manuscript.

DATA AVAILABILITY STATEMENT

Data are available from the Dryad Digital Repository https://doi.org/10.5061/dryad.9cnp5hqk5 (Bruijning et al., 2021).

ORCID

Marjolein Bruijning https://orcid.org/0000-0002-9408-2187
Erlend I. F. Fossen https://orcid.org/0000-0002-5687-2743
Eelke Jongejans https://orcid.org/0000-0003-1148-7419
Héléne Vanvelk https://orcid.org/0000-0002-7038-5239
Joost A. M. Raeymaekers https://orcid.org/0000-0003-2732-7495
Lynn Govaert https://orcid.org/0000-0001-8326-3591
Kristien I. Brans https://orcid.org/0000-0002-0464-7720
Sigurd Einum https://orcid.org/0000-0002-3788-7800
Luc De Meester https://orcid.org/0000-0001-5433-6843

REFERENCES

Alan Pounds, J., Bustamante, M. R., Coloma, L. A., Consuegra, J. A., Fogden, M. P. L., Foster, P. N., La Marca, E., Masters, K. L., Merino-Viteri, A., Puschendorf, R., Ron, S. R., Sánchez-Azofeifa, G. A., Still, C. J., & Young, B. E. (2006). Widespread amphibian extinctions from epidemic disease driven by global warming. *Nature*, *439*, 161–167. https://doi.org/10.1038/nature04246

Altizer, S., Ostfeld, R. S., Johnson, P. T. J., Kutz, S., & Harvell, C. D. (2013). Climate change and infectious diseases: From evidence to a predictive framework. *Science*, *341*, 514–519. https://doi.org/10.1126/science.1239401

Araújo, M. B., & Luoto, M. (2007). The importance of biotic interactions for modelling species distributions under climate change. *Global Ecology and Biogeography*, *16*, 743–753. https://doi.org/10.1111/j.1466-8238.2007.00359.x

Bellard, C., Bertelsmeier, C., Leadley, P., Thuiller, W., & Courchamp, F. (2012). Impacts of climate change on the future of biodiversity. *Ecology Letters*, *15*, 365–377. https://doi.org/10.1111/j.1461-0248.2011.01736.x

Bjørnstad, O. N., Finkenstädt, B. F., & Grenfell, B. T. (2002). Dynamics of measles epidemics: Estimating scaling of transmission rates using a time series SIR model. *Ecological Monographs*, *72*, 169–184.

Brambilla, D. J. (1983). Microsporidiosis in a *Daphnia pulex* population. *Hydrobiologia*, *99*, 175–188. https://doi.org/10.1007/BF00008769

Brans, K. I., Jansen, M., Vanoverbeke, J., Tüzün, N., Stoks, R., & De Meester, L. (2017). The heat is on: Genetic adaptation to urbanization mediated by thermal tolerance and body size. *Global Change Biology*, *23*, 5218–5227. https://doi.org/10.1111/gcb.13784

Bruijning, M., Fossen, E. I. F., Jongejans, E., Vanvelk, H., Raeymaekers, J. A. M., Govaert, L., Brans, K. I., Einum, S., & De Meester, L. (2021). Data from: Host–parasite dynamics shaped by temperature and genotype: Quantifying the role of underlying vital rates. *Dryad Digital Repository*, https://doi.org/10.5061/dryad.9cnp5hqk5

Bruijning, M., ten Berge, A. C. M., & Jongejans, E. (2018). Population-level responses to temperature, density and clonal differences in *Daphnia magna* as revealed by Integral Projection Modeling. *Functional Ecology*, *32*, 2407–2422.

Bruijning, M., Visser, M. D., Hallmann, C. A., & Jongejans, E. (2018). *trackdem*: Automated particle tracking to obtain population counts and size distributions from videos in R. *Methods in Ecology and Evolution*, *9*, 965–973.

Bruijning, M., Visser, M. D., Muller-Landau, H. C., Wright, S. J., Comita, L. S., Hubbell, S. P., de Kroon, H., & Jongejans, E. (2017). Surviving in a cosexual world: A cost-benefit analysis of dioecy in tropical trees. *The American Naturalist*, *189*, 297–314. https://doi.org/10.1086/690137

Carius, H. J., Little, T. J., & Ebert, D. (2001). Genetic variation in a host-parasite association: Potential for coevolution and frequency-dependent selection. *Evolution*, *55*, 1136–1145. https://doi.org/10.1111/j.0014-3820.2001.tb00633.x

Caswell, H. (1978). A general formula for the sensitivity of population growth rate to changes in life history parameters. *Theoretical Population Biology*, *14*, 215–230. https://doi.org/10.1016/0040-5809(78)90025-4

Chiavelli, D. A., Mills, E. L., & Threlkeld, S. T. (1993). Host preference, seasonality, and community interactions of zooplankton epibionts. *Limnology and Oceanography*, *38*, 574–583. https://doi.org/10.4319/lo.1993.38.3.0574

Childs, D. Z., Sheldon, B. C., & Rees, M. (2016). The evolution of labile traits in sex- and age-structured populations. *Journal of Animal Ecology*, *85*, 329–342. https://doi.org/10.1111/1365-2656.12483

Cohen, J. M., Civitello, D. J., Venesky, M. D., McMahon, T. A., & Rohr, J. R. (2019). An interaction between climate change and infectious disease drove widespread amphibian declines. *Global Change Biology*, *25*, 927–937. https://doi.org/10.1111/gcb.14489

Coulson, T., Kendall, B. E., Barthold, J., Plard, F., Schindler, S., Ozgul, A., & Gaillard, J.-M. (2017). Modeling adaptive and nonadaptive responses of populations to environmental change. *The American Naturalist*, *190*, 313–336. https://doi.org/10.1086/692542

Coulson, T., MacNulty, D. R., Stahler, D. R., VonHoldt, B., Wayne, R. K., & Smith, D. W. (2011). Modeling effects of environmental change on wolf population dynamics, trait evolution, and life history. *Science*, *334*, 1275–1278. https://doi.org/10.1126/science.1209441

Czypionka, T., Reeves, G., Vanhamel, M., & De Meester, L. (2016). Assessing hatching rates and the timing of hatching from plankton resting stages-an accurate and cost effective high throughput approach. *Limnology and Oceanography: Methods*, *14*, 718–724.

De Meester, L., Stoks, R., & Brans, K. I. (2018). Genetic adaptation as a biological buffer against climate change: Potential and limitations. *Integrative Zoology*, *13*, 372–391.

Decaestecker, E., Declerck, S., De Meester, L., & Ebert, D. (2005). Ecological implications of parasites in natural *Daphnia* populations. *Oecologia*, *144*, 382–390. https://doi.org/10.1007/s00442-005-0083-7

Decaestecker, E., Gaba, S., Raeymaekers, J. A. M., Stoks, R., Van Kerckhoven, L., Ebert, D., & De Meester, L. (2007). Host-parasite "Red Queen" dynamics archived in pond sediment. *Nature*, *450*, 870–873. https://doi.org/10.1038/nature06291

Decaestecker, E., Lefever, C., De Meester, L., & Ebert, D. (2004). Haunted by the past: Evidence for dormant stage banks of microparasites and epibionts of *Daphnia*. *Limnology and Oceanography*, *49*, 1355–1364. https://doi.org/10.4319/lo.2004.49.4_part_2.1355

Dell, A. I., Pawar, S., & Savage, V. M. (2011). Systematic variation in the temperature dependence of physiological and ecological traits. *Proceedings of the National Academy of Sciences of the United States of America*, *108*, 10591–10596. https://doi.org/10.1073/pnas.1015178108

Easterling, M. R., Ellner, S. P., & Dixon, P. M. (2000). Size-specific sensitivity: Applying a new structured population model. *Ecology*, *81*, 694–708.

Ebert, D. (1995). The ecological interactions between a microsporidian parasite and its host *Daphnia magna*. *The Journal of Animal Ecology*, *64*, 361. https://doi.org/10.2307/5897

Ebert, D. (2005). Ecology, epidemiology, and evolution of parasitism in *Daphnia*.

Ebert, D., Zschokke-Rohringer, C. D., & Carius, H. J. (2000). Dose effects and density-dependent regulation of two microparasites of *Daphnia magna*. *Oecologia*, *122*, 200–209. https://doi.org/10.1007/PL00008847

Ellner, S. P., Childs, D. Z., & Rees, M. (2016). *Data-driven modelling of structured populations. A Practical Guide to the Integral Projection Model*. Springer International Publishing.

Ellner, S. P., & Rees, M. (2006). Integral projection models for species with complex demography. *The American Naturalist*, *167*, 410–428. https://doi.org/10.1086/499438

Ficke, A. D., Myrick, C. A., & Hansen, L. J. (2007). Potential impacts of global climate change on freshwater fisheries. *Reviews in Fish Biology and Fisheries*, *17*, 581–613. https://doi.org/10.1007/s11160-007-9059-5

Geerts, A. N., Vanoverbeke, J., Vanschoenwinkel, B., Van Doorslaer, W., Feuchtmayr, H., Atkinson, D., Moss, B., Davidson, T. A., Sayer, C. D., & De Meester, L. (2015). Rapid evolution of thermal tolerance in the water flea *Daphnia*. *Nature Climate Change*, *5*, 665–668.

Gehman, A.-L.- M., Hall, R. J., & Byers, J. E. (2018). Host and parasite thermal ecology jointly determine the effect of climate warming on epidemic dynamics. *Proceedings of the National Academy of Sciences of the United States of America*, *115*, 744–749. https://doi.org/10.1073/pnas.1705067115

Giebelhausen, B., & Lampert, W. (2001). Temperature reaction norms of *Daphnia magna*: The effect of food concentration. *Freshwater Biology*, *46*, 281–289.

Gilman, S. E., Urban, M. C., Tewksbury, J., Gilchrist, G. W., & Holt, R. D. (2010). A framework for community interactions under climate change. *Trends in Ecology & Evolution*, *25*, 325–331. https://doi.org/10.1016/j.tree.2010.03.002

Goser, B., & Ratte, H. T. (1994). Experimental evidence of negative interference in *Daphnia magna*. *Oecologia*, *98*, 354–361. https://doi.org/10.1007/BF00324224

Greenspan, S. E., Bower, D. S., Roznik, E. A., Pike, D. A., Marantelli, G., Alford, R. A., Schwarzkopf, L., & Scheffers, B. R. (2017). Infection increases vulnerability to climate change via effects on host thermal tolerance. *Scientific Reports*, *7*, 1–10. https://doi.org/10.1038/s41598-017-09950-3

Guisande, C. (1993). Reproductive strategy as population density varies in *Daphnia magna* (Cladocera). *Freshwater Biology*, *29*, 463–467. https://doi.org/10.1111/j.1365-2427.1993.tb00780.x

Hall, S. R., Tessier, A. J., Duffy, M. A., Huebner, M., & Cáceres, C. E. (2006). Warmer does not have to mean sicker: Temperature and predators can jointly drive timing of epidemics. *Ecology*, *87*, 1684–1695.

Harvell, C. D., Mitchell, C. E., Ward, J. R., Altizer, S., Dobson, A. P., Ostfeld, R. S., & Samuel, M. D. (2002). Climate warming and disease risks for terrestrial and marine biota. *Science*, *296*, 2158–2162. https://doi.org/10.1126/science.1063699

Hector, T. E., Sgrò, C. M., & Hall, M. D. (2019). Pathogen exposure disrupts an organism's ability to cope with thermal stress. *Global Change Biology*, *25*, 3893–3905. https://doi.org/10.1111/gcb.14713

Heikkinen, R. K., Luoto, M., Virkkala, R., Pearson, R. G., & Körber, J.-H. (2007). Biotic interactions improve prediction of boreal bird distributions at macro-scales. *Global Ecology and Biogeography*, *16*, 754–763. https://doi.org/10.1111/j.1466-8238.2007.00345.x

Henning-Lucass, N., Cordellier, M., Streit, B., & Schwenk, K. (2016). Phenotypic plasticity in life-history traits of *Daphnia galeata* in response to temperature—A comparison across clonal lineages separated in time. *Ecology and Evolution*, *6*, 881–891.

Hickling, R., Roy, D. B., Hill, J. K., Fox, R., & Thomas, C. D. (2006). The distributions of a wide range of taxonomic groups are expanding polewards. *Global Change Biology*, *12*, 450–455. https://doi.org/10.1111/j.1365-2486.2006.01116.x

Hoffmann, A. A., & Sgrò, C. M. (2011). Climate change and evolutionary adaptation. *Nature*, *470*, 479–485. https://doi.org/10.1038/nature09670

Huey, R. B., & Kingsolver, J. G. (2019). Climate warming, resource availability, and the metabolic meltdown of ectotherms. *The American Naturalist*, *194*, E140–E150.

Kirk, D., Jones, N., Peacock, S., Phillips, J., Molnár, P. K., Krkošek, M., & Luijckx, P. (2018). Empirical evidence that metabolic theory describes the temperature dependency of within-host parasite dynamics. *PLoS Biology*, *16*, e2004608. https://doi.org/10.1371/journal.pbio.2004608

Kirk, D., Luijckx, P., Jones, N., Krichel, L., Pencer, C., Molnár, P., & Krkošek, M. (2020). Experimental evidence of warming-induced disease emergence and its prediction by a trait-based mechanistic model. *Proceedings of the Royal Society B: Biological Sciences*, *287*(1936), 20201526. https://doi.org/10.1098/rspb.2020.1526

Kuno, G. (1973). Biological notes of *Amoebidium parasiticum* found in Puerto Rico. *Journal of Invertebrate Pathology*, *21*, 1–8. https://doi.org/10.1016/0022-2011(73)90105-5

Labaude, S., Rigaud, T., & Cézilly, F. (2017). Additive effects of temperature and infection with an acanthocephalan parasite on the shredding activity of *Gammarus fossarum* (Crustacea: Amphipoda): The importance of aggregative behavior. *Global Change Biology*, *23*, 1415–1424.

Lafferty, K. D. (2009). The ecology of climate change and infectious diseases. *Ecology*, *90*, 888–900. https://doi.org/10.1890/08-0079.1

Lafferty, K. D., & Mordecai, E. A. (2016). The rise and fall of infectious disease in a warmer world. *F1000Research*, *5*, 2040. https://doi.org/10.12688/f1000research.8766.1

Lampert, W. (1978). A field study on the dependence of the fecundity of *Daphnia spec*. on food concentration. *Oecologia*, *36*, 363–369. https://doi.org/10.1007/BF00348062

Little, T. J., Shuker, D. M., Colegrave, N., Day, T., & Graham, A. L. (2010). The coevolution of virulence: Tolerance in perspective. *PLoS Path*, *6*, e1001006. https://doi.org/10.1371/journal.ppat.1001006

MacArthur, J. W., & Baillie, W. H. T. (1929). Metabolic activity and duration of life. I. Influence of temperature on longevity in *Daphnia magna*. *Journal of Experimental Zoology*, *53*, 221–242.

Merow, C., Dahlgren, J. P., Metcalf, C. J. E., Childs, D. Z., Evans, M. E. K., Jongejans, E., Record, S., Rees, M., Salguero-Gómez, R., &

McMahon, S. M. (2014). Advancing population ecology with integral projection models: A practical guide. *Methods in Ecology and Evolution*, *5*, 99–110. https://doi.org/10.1111/2041-210X.12146

Metcalf, C. J. E., Graham, A. L., Martinez-Bakker, M., & Childs, D. Z. (2016). Opportunities and challenges of Integral Projection Models for modelling host-parasite dynamics. (R. Salguero-Gómez, ed.). *Journal of Animal Ecology*, *85*, 343–355. https://doi.org/10.1111/1365-2656.12456

Metcalf, C. J. E., Rose, K. E., Childs, D. Z., Sheppard, A. W., Grubb, P. J., & Rees, M. (2008). Evolution of flowering decisions in a stochastic, density-dependent environment. *Proceedings of the National Academy of Sciences of the United States of America*, *105*, 10466–10470. https://doi.org/10.1073/pnas.0800777105

Mokany, K., Bush, A., & Ferrier, S. (2019). Community assembly processes restrict the capacity for genetic adaptation under climate change. *Ecography*, *42*, 1164–1174. https://doi.org/10.1111/ecog.03994

Mordecai, E. A., Caldwell, J. M., Grossman, M. K., Lippi, C. A., Johnson, L. R., Neira, M., Rohr, J. R., Ryan, S. J., Savage, V., Shocket, M. S., Sippy, R., Stewart Ibarra, A. M., Thomas, M. B., & Villena, O. (2019). Thermal biology of mosquito-borne disease. *Ecology Letters*, *22*, 1690–1708. https://doi.org/10.1111/ele.13335

Morley, N. J., & Lewis, J. W. (2014). Temperature stress and parasitism of endothermic hosts under climate change. *Trends in Parasitology*, *30*, 221–227. https://doi.org/10.1016/j.pt.2014.01.007

Mouritsen, K. N., Tompkins, D. M., & Poulin, R. (2005). Climate warming may cause a parasite-induced collapse in coastal amphipod populations. *Oecologia*, *146*, 476–483. https://doi.org/10.1007/s00442-005-0223-0

Ockendon, N., Baker, D. J., Carr, J. A., White, E. C., Almond, R. E. A., Amano, T., Bertram, E., Bradbury, R. B., Bradley, C., Butchart, S. H. M., Doswald, N., Foden, W., Gill, D. J. C., Green, R. E., Sutherland, W. J., Tanner, E. V. J., & Pearce-Higgins, J. W. (2014). Mechanisms underpinning climatic impacts on natural populations: Altered species interactions are more important than direct effects. *Global Change Biology*, *20*, 2221–2229. https://doi.org/10.1111/gcb.12559

Oli, M. K., Venkataraman, M., Klein, P. A., Wendland, L. D., & Brown, M. B. (2006). Population dynamics of infectious diseases: A discrete time model. *Ecological Modelling*, *198*, 183–194. https://doi.org/10.1016/j.ecolmodel.2006.04.007

Orsini, L., Spanier, K. I., & De Meester, L. (2012). Genomic signature of natural and anthropogenic stress in wild populations of the waterflea *Daphnia magna*: Validation in space, time and experimental evolution. *Molecular Ecology*, *21*, 2160–2175.

Ozgul, A., Childs, D. Z., Oli, M. K., Armitage, K. B., Blumstein, D. T., Olson, L. E., Tuljapurkar, S., & Coulson, T. (2010). Coupled dynamics of body mass and population growth in response to environmental change. *Nature*, *466*, 482–485. https://doi.org/10.1038/nature09210

Ozgul, A., Coulson, T., Reynolds, A., Cameron, T. C., & Benton, T. G. (2012). Population responses to perturbations: The importance of trait-based analysis illustrated through a microcosm experiment. *The American Naturalist*, *179*, 582–594. https://doi.org/10.1086/664999

Padfield, D., Castledine, M., & Buckling, A. (2020). Temperature-dependent changes to host–parasite interactions alter the thermal performance of a bacterial host. *The ISME Journal*, *14*, 389–398. https://doi.org/10.1038/s41396-019-0526-5

Pauwels, K., Stoks, R., Decaestecker, E., & De Meester, L. (2007). Evolution of heat shock protein expression in a natural population of *Daphnia magna*. *The American Naturalist*, *170*, 800–805.

Råberg, L., Sim, D., Read, A. F., & Raberg, L. (2007). Disentangling genetic variation for resistance and tolerance to infectious diseases in animals. *Science*, *318*, 812–814. https://doi.org/10.1126/science.1148526

Salguero-Gomez, R., Siewert, W., Casper, B. B., & Tielbörger, K. (2012). A demographic approach to study effects of climate change in desert plants. *Philosophical Transactions of the Royal Society B: Biological Sciences*, *367*, 3100–3114. https://doi.org/10.1098/rstb.2012.0074

Schäfer, R. B., & Piggott, J. J. (2018). Advancing understanding and prediction in multiple stressor research through a mechanistic basis for null models. *Global Change Biology*, *24*, 1817–1826. https://doi.org/10.1111/gcb.14073

Shocket, M., Magnante, A., Duffy, M., Caceres, C., & Hall, S. (2019). Can hot temperatures limit disease transmission? A test of mechanisms in a zooplankton-fungus system. *Functional Ecology*, *33*, 2017–2029. https://doi.org/10.1111/1365-2435.13403

Shocket, M. S., Strauss, A. T., Hite, J. L., Šljivar, M., Civitello, D. J., Duffy, M. A., Cáceres, C. E., & Hall, S. R. (2018). Temperature drives epidemics in a zooplankton-fungus disease system: A trait-driven approach points to transmission via host foraging. *The American Naturalist*, *191*, 435–451. https://doi.org/10.1086/696096

Smallegange, I. M., Caswell, H., Toorians, M. E. M., & de Roos, A. M. (2017). Mechanistic description of population dynamics using dynamic energy budget theory incorporated into integral projection models. *Methods in Ecology and Evolution*, *8*, 146–154. https://doi.org/10.1111/2041-210X.12675

Smallegange, I. M., & Ens, H. M. (2018). Trait-based predictions and responses from laboratory mite populations to harvesting in stochastic environments. *Journal of Animal Ecology*, *87*, 893–905. https://doi.org/10.1111/1365-2656.12802

Stearns, S. C. (1989). Trade-offs in life-history evolution. *Functional Ecology*, *3*, 259–268. https://doi.org/10.2307/2389364

Stirnadel, H. A., & Ebert, D. (1997). Prevalence, host specificity and impact on host fecundity of microparasites and epibionts in three sympatric Daphnia species. *Journal of Animal Ecology*, *66*, 212.

Tekin, E., Diamant, E. S., Cruz-Loya, M., Enriquez, V., Singh, N., Savage, V. M., & Yeh, P. J. (2020). Using a newly introduced framework to measure ecological stressor interactions. *Ecology Letters*, https://doi.org/10.1111/ele.13533

Thomas, C. D., & Lennon, J. J. (1999). Birds extend their ranges northwards. *Nature*, *399*, 213. https://doi.org/10.1038/20335

Traill, L. W., Schindler, S., & Coulson, T. (2014). Demography, not inheritance, drives phenotypic change in hunted bighorn sheep. *Proceedings of the National Academy of Sciences of the United States of America*, *111*, 13223–13228. https://doi.org/10.1073/pnas.1407508111

Tylianakis, J. M., Didham, R. K., Bascompte, J., & Wardle, D. A. (2008). Global change and species interactions in terrestrial ecosystems. *Ecology Letters*. https://doi.org/10.1111/j.1461-0248.2008.01250.x

Urban, M. C., Bocedi, G., Hendry, A. P., Mihoub, J.-B., Pe'er, G., Singer, A., Bridle, J. R., Crozier, L. G., De Meester, L., Godsoe, W., Gonzalez, A., Hellmann, J. J., Holt, R. D., Huth, A., Johst, K., Krug, C. B., Leadley, P. W., Palmer, S. C. F., Schmitz, A., … Travis, J. M. J. (2016). Improving the forecast for biodiversity under climate change. *Science*, *353*(6304), aad8466. https://doi.org/10.1126/science.aad8466

Urban, M. C., De Meester, L., Vellend, M., Stoks, R., & Vanoverbeke, J. (2012). A crucial step toward realism: Responses to climate change from an evolving metacommunity perspective. *Evolutionary Applications*, *5*, 154–167. https://doi.org/10.1111/j.1752-4571.2011.00208.x

van Buuren, S., & Groothuis-Oudshoorn, K. (2011). {mice}: Multivariate imputation by chained equations in R. *Journal of Statistical Software*, *45*, 1–67.

Van Doorslaer, W., Stoks, R., Duvivier, C., Bednarshka, A., & De Meester, L. (2009). Population dynamics determine genetic adaptation to temperature in *Daphnia*. *Evolution*, *63*, 1867–1878.

Van Doorslaer, W., Vanoverbeke, J., Duvivier, C., Rousseaux, S., Jansen, M., Jansen, B., Feuchtmayr, H., Atkinson, D., Moss, B., Stoks, R., & De Meester, L. (2009). Local adaptation to higher temperatures reduces immigration success of genotypes from a warmer region in the water flea Daphnia. *Global Change Biology*, *15*, 3046–3055.

Vindenes, Y., & Langangen, Ø. (2015). Individual heterogeneity in life histories and eco-evolutionary dynamics. *Ecology Letters*, *18*, 417–432. https://doi.org/10.1111/ele.12421

Wilber, M. Q., Langwig, K. E., Kilpatrick, A. M., McCallum, H. I., & Briggs, C. J. (2016). Integral Projection Models for host-parasite systems with an application to amphibian chytrid fungus. (J. Metcalf, ed.). *Methods in Ecology and Evolution*, *7*, 1182–1194. https://doi.org/10.1111/2041-210X.12561

Yampolsky, L. Y., Schaer, T. M. M., & Ebert, D. (2014). Adaptive phenotypic plasticity and local adaptation for temperature tolerance in freshwater zooplankton. *Proceedings of the Royal Society B: Biological Sciences*, *281*(1776), 20132744. https://doi.org/10.1098/rspb.2013.2744

Yuan, Y. C. (2000). *Multiple imputation for missing data: Concepts and new development (version 9.0)* (pp. 1–13). SUGI Proceedings.

SUPPORTING INFORMATION

Additional supporting information may be found in the online version of the article at the publisher's website.

How to cite this article: Bruijning, M., Fossen, E. I. F., Jongejans, E., Vanvelk, H., Raeymaekers, J. A. M., Govaert, L., Brans, K. I., Einum, S., & De Meester, L. (2022). Host–parasite dynamics shaped by temperature and genotype: Quantifying the role of underlying vital rates. *Functional Ecology*, 36, 485–499. https://doi.org/10.1111/1365-2435.13966